

UNIVERSITY OF FLORENCE
School of Engineering

Master degree program in
COMPUTER ENGINEERING

Disparity coherent stereo video watermarking

Master Thesis of
Benedetta Barbetti, Michaela Servi
December 2015

Supervisor:

Prof. Alessandro Piva

Advisors:

Prof. Carlo Colombo
Dott. Pasquale Ferrara
Dott. Francesca Uccheddu

Academic Year 2014/2015

Abstract

Contents

Introduction	1
1 Stereoscopic Video	3
1.1 Stereo vision	5
1.1.1 Acquisition of stereoscopic images	6
1.1.2 Disparity map computation	8
1.2 3D capturing devices	12
1.3 3D video displays	15
2 Stereo video watermarking	17
2.1 Watermaking	17
2.1.1 Properties	18
2.1.2 Embedding techniques	20
2.1.3 Embedding domains	21
3 Frequency disparity-coherent watermarking	24
3.1 ALGORITMO DEL PROF	24
3.1.1 Watermark embedding	25
3.1.2 Watermark detection	25
3.2 Stereo watermarking algorithm	27
3.3 Stereo detection algorithm	28

4 Conclusions	30
Bibliografia	31

List of Figures

1.1	Stereoscopy in medical and industrial field	4
1.2	Stereoscopy application's fields	4
1.3	Stereoscopy in 3D video games	5
1.4	Binocular human vision vs. stereoscopic content acquisition.	6
1.5	Triangulation: with two cameras the depth of	6
1.6	Stereo camera model	7
1.7	Rectified stereo cameras	8
1.8	Rectified images: corresponding points (p, p'), projection of the same 3D point (P) are constrained on the same image horizontal line, the epipolar line	8
1.9	Geometry of standard form	9
1.10	Stereo pair and disparity map	10
1.11	Stereo matching general problems	10
1.12	Local stereo matching, window based	11
1.13	Results of the Kolmogorov and Zabih's graph cuts algorithm on the Tsukuba pair	12
1.14	Interaxial separation between lenses	12
1.15	Professional technologies for 3D TV	13
1.16	Digital personal stereo vision systems	14
1.17	Industrial and robotic stereo cameras	14

1.18	Passive and active glasses for 3D viewer technologies	16
2.1	Watermarking workflow	17
2.2	Watermark properties trade-off	18
2.3	Spread spectrum technique	20
2.4	Side information technique scheme	21
2.5	Spatial domain watermark insertion	21
2.6	Frequency domain watermark insertion	22
2.7	Hybrid technique	22
2.8	Stereoscopic video watermarking workflow	23

List of Tables

Introduction

In the last few years the stereoscopic technique has become a great part of image and video processing.

In medical diagnosis and endoscopic surgery as in fault detection in manufactory industry, army and arts, multiview imaging is considered as a key enabler for professional added value services.

Nowdays stereoscopic techniques are also used in people tracking and mobile robotics navigation for economic reasons and to improve performances.

Finally the worldwide success of 3D movie releases and 3D video games and the deployment of 3D televisions made the nonprofessional user aware about a new type of multimedia entertainment experience.

The increasing production and distribution of these contents leads to the concerns over copyright protection.

Digital watermarking can be considered as the most flexible property right protection technology, since it adds some information (a mark, i.e. copyright information) in the original content without altering its visual quality so that such a marked content can be further distributed/consumed by another user without any restriction; still, the legitimate/illegitimate usage can be determined at any moment by detecting the mark. In same case the watermarking protection mechanism, instead of restricting the media copy/distribution/consumption, provides means for tracking the source of

the content illegitimate usage.

The purpose of this thesis is to provide a new watermarking system for copyright protection of stereoscopic videos.

The method operates in the frequency and in the spatial domain by embedding a pseudo-random sequence of real numbers in a selected set of DFT coefficients of the left image; then the reference watermark is distorted according to the depth information prior to insertion and spatially added to the right image.

In Chapter ??...

Chapter 1

Stereoscopic Video

In a wide variety of image processing applications, explicit depth information is required in addition to general image informations, such as intensities, color, densities.

Examples of such applications are found in 3D vision (robot vision, photogrammetry, remote sensing systems), in medical imaging (computer tomography, magnetic resonance imaging, microsurgery), in remote handling of objects (random bin picking), in space exploration (mobile robotics navigation) or 3D movies and videogames.

In each of these cases, depth information is essential for accurate image analysis or for enhancing the realism.

In remote sensing the terrain's elevation needs to be accurately determined for map production, in remote handling an operator needs to have precise knowledge of the threedimensional organization of the area to avoid collisions and misplacements.

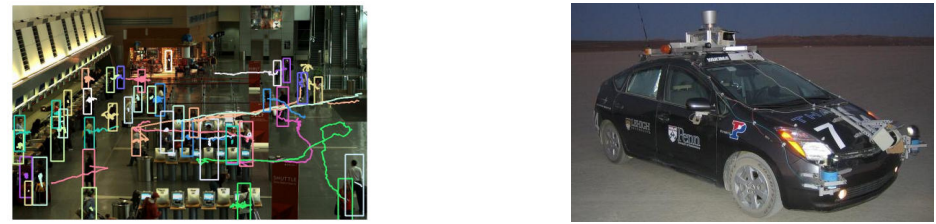
Depth in real world scenes can be explicitly measured by a number of range sensing devices such as by laser range sensors, by structured light or



(a) In bin picking applications stereo vision helps to reconstruct the 3D environment and detect the part of the object to be robotically picked

(b) Surgical robot *Da vinci* is provided with a stereoscopic camera that allows a tridimensional view of the operative field.

Figure 1.1: Stereoscopic vision in medical and industrial field



(a) In people tracking application stereo vision improves segmentation thanks to depth information and it's less sensible to light changes.

(b) In mobile robotics navigation stereo vision has became the first choice technology because it provides a lot of quality data for low costs.

Figure 1.2: Stereoscopic vision application's fields

by ultrasound. However it's usually undesirable to have separate systems for acquiring the intensity and the depth information because of the relative low resolution of the range sensing devices and because it's not an easy task to fuse information from different type of sensors; for these reasons and for a non-negligible economic factor stereoscopic vision has becoming the technology of choice in these type of applications.

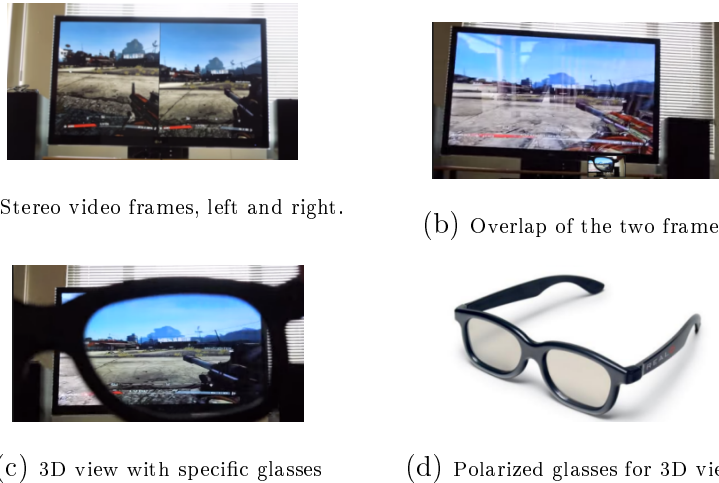


Figure 1.3: Stereoscopy in 3D video games

1.1 Stereo vision

In image processing stereo vision is the process of extracting 3D information from multiple 2D views of a scene.

The 3D information can be obtained from a pair of images, also known as a stereo pair, by estimating the relative depth of points in the scene.

From the anatomic point of view, the human brain calculates the depth in a visual scene mainly by processing the information brought by the images seen by the left and the right eyes. These left and right images are slightly different because the eyes have biologically different emplacements.

Consequently, the straightforward way of achieving stereoscopic digital imaging is to emulate the Human Visual System (HSV) by setting-up (under controlled geometric positions), two traditional 2D cameras.

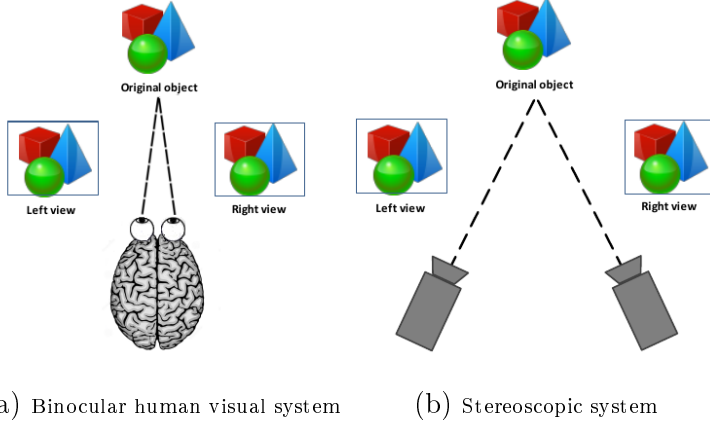


Figure 1.4: Binocular human vision vs. stereoscopic content acquisition.

1.1.1 Acquisition of stereoscopic images

In order to be able to perceive depth using recorded images, a stereoscopic camera is required, which consists of two cameras that capture two different, horizontally shifted perspective viewpoints; with two (or more) cameras we can infer depth, by means of triangulation, if we are able to find corresponding points in the two images (Figure 1.5).

The camera setup should be geometrically calibrated such that the two

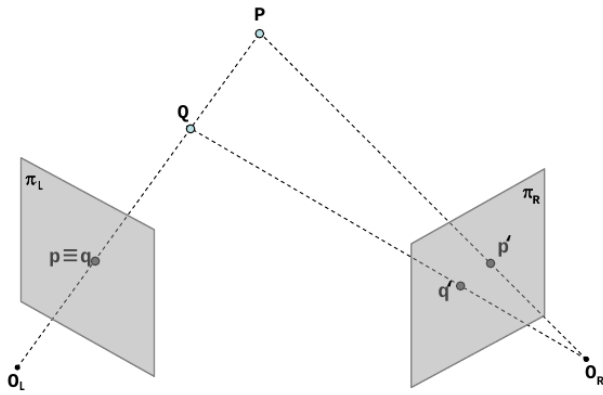


Figure 1.5: Triangulation: with two cameras the depth of

cameras capture the same part of the real world scene.

Calibration of a stereo camera system involves the estimation of the intrinsic and extrinsic parameters of the model: intrinsic parameters embody the characteristics of the optical system and its geometric relationship with the image sensor, extrinsic parameters relate the location and orientation of the second camera with respect to the first one in the 3D space (Figure 1.6).

These parameters can be used to rectify a stereo pair of images to make

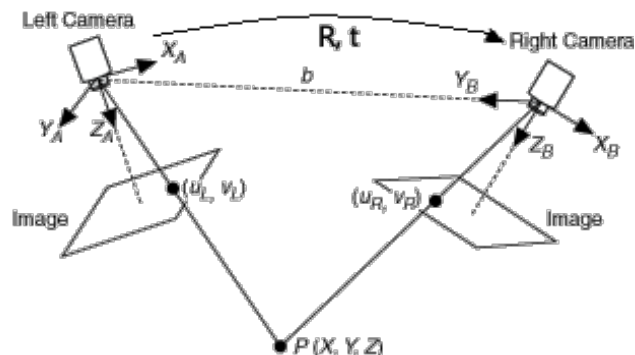


Figure 1.6: Stereo camera model

them appear as the two image planes are parallel (Figure 1.7); once the images are rectified, epipolar geometry it's used to find corresponding points and compute the disparity map.

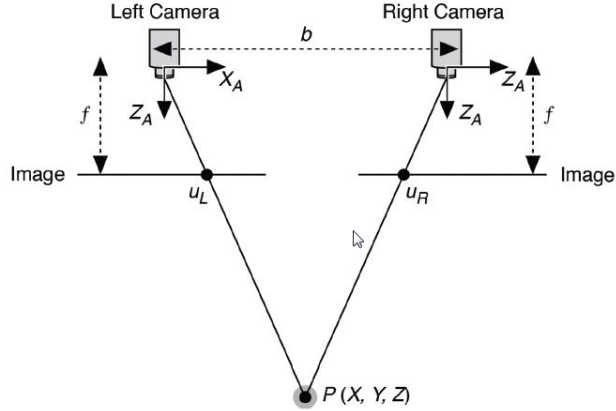
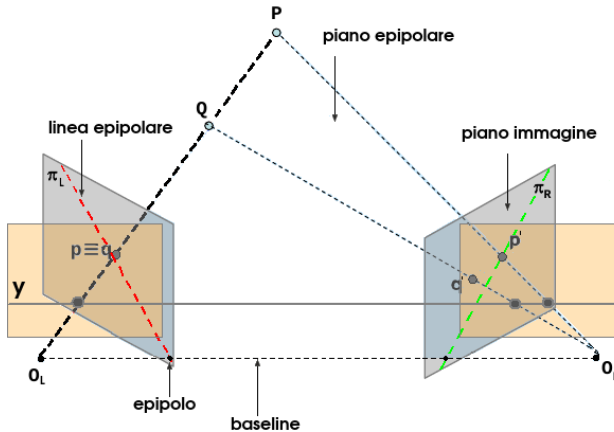


Figure 1.7: Rectified stereo cameras

Figure 1.8: Rectified images: corresponding points (p, p'), projection of the same 3D point (P) are constrained on the same image horizontal line, the epipolar line

1.1.2 Disparity map computation

With the stereo rig in standard form and by considering similar triangles in Figure 1.9 ($PO_L O_R$ and $Pp p'$):

$$\frac{b}{Z} = \frac{(b + x_L) - x_R}{Z - f}$$

so

$$Z = \frac{b \cdot f}{x_L - x_R} = \frac{b \cdot f}{d}$$

where $d = x_L - x_R$ it's called *disparity*.

Disparity is, therefore, the difference between the x coordinates of two cor-

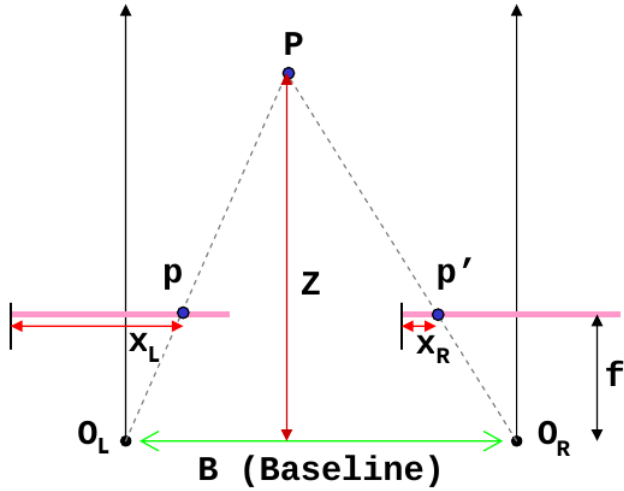


Figure 1.9: Geometry of standard form

responding points and it is usually encoded with greyscale image (Figure 1.10c), where points closer to the cameras are brighter and correspond to a higher disparity.

In order to compute the disparity map is necessary to find corresponding points; stereo correspondance is though a challenging task that has to manage with perspective distortions, uniform and ambiguous regions, repetitive patterns, occlusions and discontinuities(Figure 1.11).

In general, stereo matching algorithms can be categorized into two major classes:

- local methods

- global methods.

Local stereo algorithms estimate the correspondence using a local support region or a window. Local algorithms generally rely on an approximation

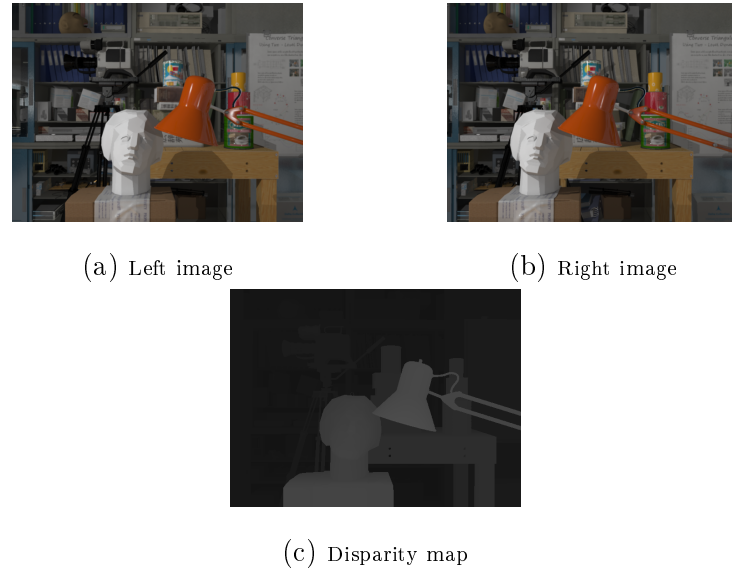


Figure 1.10: Stereo pair and disparity map

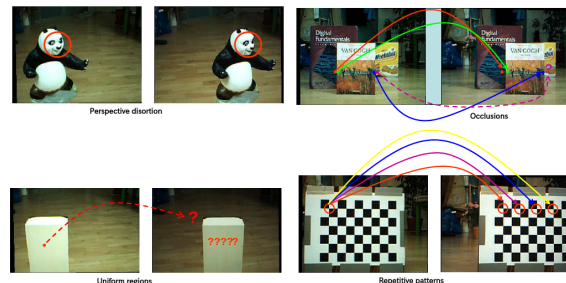


Figure 1.11: Stereo matching general problems

of the smoothness constraint assuming that all pixels within the matching region have the same disparity. However, this assumption is not valid for highly curved surfaces or around disparity discontinuities.

A naive approach consists of comparing each pixel or window in the left image with every pixel or window on the same epipolar line in right image and picking position with minimum match cost (e.g., SSD, SAD, normalized correlation).

Global stereo methods consider stereo matching as a labeling problem where

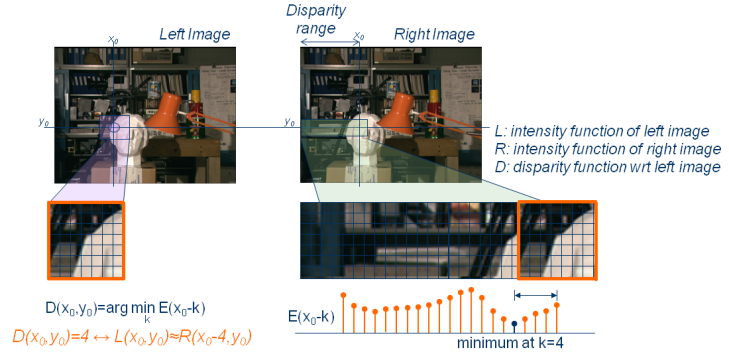


Figure 1.12: Local stereo matching, window based

the pixels of the reference image are nodes and the estimated disparities are labels. An energy functional embeds the matching assumptions by its data, smoothness, and occlusion terms and propagates them along the scan line or through the whole image. The labeling problem is solved by energy functional minimization, using dynamic programming, graph cuts, or belief propagation.

Even if this class of algorithms is significantly slow, the results, especially when textures and discontinuities are present, are much accurate.

In this thesis the Kolmogorov and Zabih's Graph Cuts Stereo Matching Algorithm has been used, because there were no time constraints requirements and the quality of the computed disparities has been considered satisfying with regard to the ground truth.

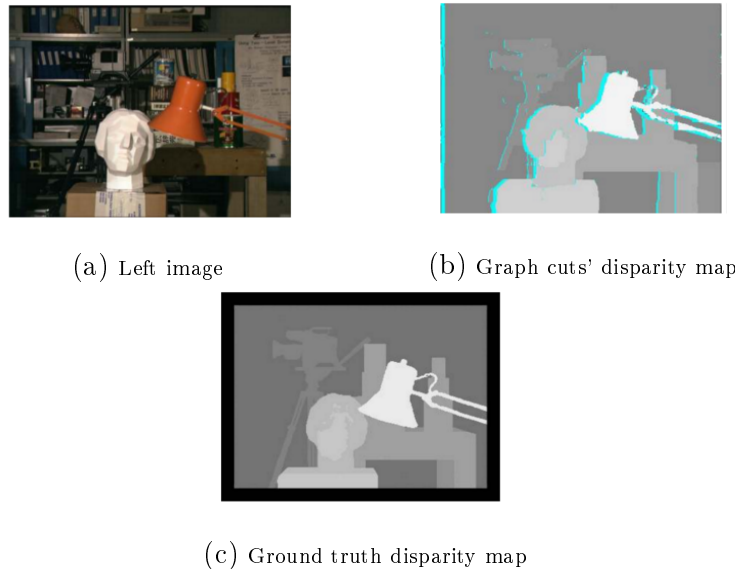


Figure 1.13: Results of the Kolmogorov and Zabih's graph cuts algorithm on the Tsukuba pair

1.2 3D capturing devices

For stereoscopic shooting, two synchronized cameras must be used. The distance between the center of the lenses of the two cameras is called the interaxial, and the cameras' convergence, is called the angulation. These two parameters can be modified according to the expected content peculiarities.

The two cameras must be correctly aligned, identically calibrated (i.e.



Figure 1.14: Interaxial separation between lenses

brightness, color, etc...) and perfectly synchronized (frame-rate and scan-

wise).

To hold and align the cameras, a stereo-rig is used; the rigs can be of two main types:

- the side-by-side rig, where the cameras are placed side by side (Figure 1.15a). This kind of 3D-rig is mostly useful for large landscape shots since it allows large interaxials; however, it doesn't allow small interaxials because of the physical size of the cameras;

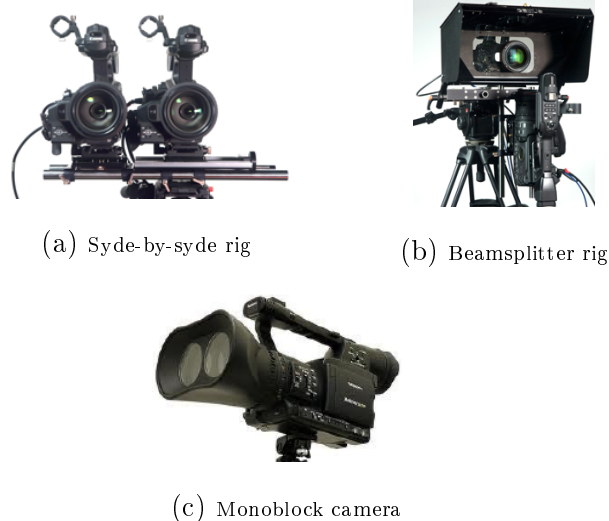


Figure 1.15: Professional technologies for 3D TV

- the beamsplitter rig (Figure 1.15b), where one camera films through a semi-transparent mirror, and the other films the reflection in the mirror. These rigs allow small and medium interaxials, useful for most shots, but not the very large interaxials (because the equipment would be too large and heavy).

Monoblock cameras have been designed as well, where the two cameras are presented in a fixed block and are perfectly aligned, which avoids cameras desynchronization (Figure 1.15c).

A second category of 3D shooting devices is presented in Figure 1.16. These electronic devices are less expensive and are targeting the user-created stereoscopic picture/movie distribution.

An other important category of 3D image capture devices it's the one em-



Figure 1.16: Digital personal stereo vision systems

ployed in the robotics and automation field. They are usually impressively precise, cost-efficient and fast.

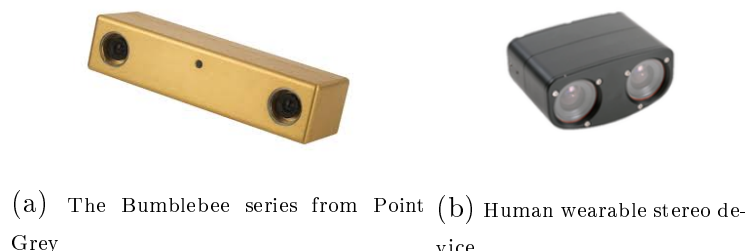


Figure 1.17: Industrial and robotic stereo cameras

1.3 3D video displays

The basic technique of stereo displays is to present offset images that are displayed separately to the left and right eye. Both of these 2D offset images are then combined in the brain to give the perception of 3D depth.

For stereoscopic 3D displays the viewer needs to wear special glasses which separate the views of the stereoscopic image for the left and the right eye. These 3D glasses can be active or passive.

On the one hand, active glasses are controlled by a timing signal that allows to alternatively darken one eye glass, and then the other, in synchronization with the refresh rate of the screen. Hence presenting the image intended for the left eye while blocking the right eye's view, then presenting the right-eye image while blocking the left eye, and repeating the process at a high speed which gives the perception of a single 3D image. This technology generally uses liquid crystal shutter glasses(Figure 1.18a).

On the other hand, passive glasses are polarization-based systems and contain a pair of opposite polarizing filters; each of them passes light with similar polarization and blocks the opposite polarized light (Figure 1.18b). Passive 3D TV screens sport a filter with alternating horizontal and vertical stripes, separated by a black, picture-blanking bars. When used with glasses which have corresponding polarising lenses, alternate frames are presented to each eye to create a 3D image.

The color anaglyph-based systems are a particular case of the passive glasses and use a color filter for each eye, typically red and cyan, Figure 1.18c . The anaglyph 3D image contains two images encoded using the same color filter, thus ensuring that each image reaches only one eye.



(a) LCD shutter glasses



(b) Polarized glasses



(c) Anaglyph glasses

Figure 1.18: Passive and active glasses for 3D viewer technologies

Chapter 2

Stereo video watermarking

2.1 Watermarking

Digital watermarking consists in imperceptibly and persistently associating some extra information with some original content.

The basic watermarking workflow is presented in Figure 2.1.

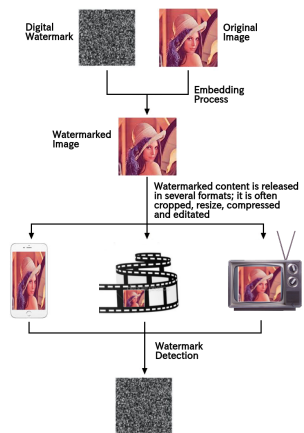


Figure 2.1: Watermarking workflow

2.1.1 Properties

Three parameters are required to evaluate watermarking technique performances:

- transparency, that is the measure of how much the watermark affects the quality of the host data;
- robustness, i.e., the capability of the hidden data to survive host signal manipulation including compression, signal processing, geometric manipulations;
- data payload, that is the amount of data of information bits that it is able to convey.

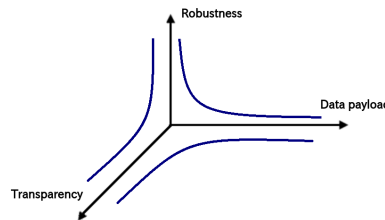


Figure 2.2: Watermark properties trade-off

To evaluate the quality of the watermarking technique in terms of transparency the measures in [3] have been used.

In Chaminda et al.'s study a Reduced-Reference (RR) quality metric for color plus depth 3D video compression and transmission is proposed, using the extracted edge information of color plus depth map 3D video.

The work is motivated by the fact that the edges/contours of the depth map can represent different depth levels and this can be considered for measuring structural degradations. Since depth map boundaries are also coincident with the corresponding color image object boundaries, edge information of

the color image and of the depth map is compared to obtain a quality index (structural degradation) for the corresponding color image sequence.

In order to quantify structural comparison, luminance comparison and contrast comparison parameters for the depth map and corresponding watermarked views, a modified version of the commonly used SSIM metric is adopted:

$$Q_{Depth}(x, y) = [l(x, y)]^\alpha \cdot [c(x, y)]^\beta \cdot [S_{Depth}(x', y')]^\gamma \quad (2.1)$$

where $l(x, y)$ and $c(x, y)$ are luminance and contrast comparisons performed on original depth maps and the ones computed after watermarking, respectively, and $S_{Depth}(x', y')$ is the structural comparison between the gradient/edge maps of original and post-watermarking computed depth map images.

Then the overall depth map quality is calculated as

$$MQ_{Depth}(X, Y) = \frac{1}{M} \sum_{j=1}^M Q_{Depth}(x_j, y_j). \quad (2.2)$$

The SSIM-based quality index for the color image can be described as follows:

$$Q_{View}(x, y) = [l(x, y)]^\alpha \cdot [c(x, y)]^\beta \cdot [S_{View}(x', y')]^\gamma \quad (2.3)$$

where $l(x, y)$ and $c(x, y)$ are luminance and contrast comparisons performed on original and watermarked views, respectively, and $S_{View}(x', y')$ is the structural comparison between the gradient/edge maps of the gradient maps of the corresponding original depth map and the watermarked views.

Hence, the overall color image quality is calculated as

$$MQ_{View}(X, Y) = \frac{1}{M} \sum_{j=1}^M Q_{View}(x_j, y_j). \quad (2.4)$$

As in [3], the Sobel operator has been selected to obtain edge information (i.e., the binary edge mask) due to its simplicity and efficiency.

Since in stereoscopic video context it is rather common practice to generate intermediate virtual views to adjust depth perception and since such view synthesis introduces non-rigid local geometric distortion that are not properly tackled by state-of-the art resynchronization mechanisms, stereo video watermarking strategies have to achieve robustness to synthetic view synthesis.

In this thesis a disparity-coherent method has been implemented since this class of watermarking technique are expected to exhibit superior robustness against view synthesis.

2.1.2 Embedding techniques

The most straightforward ways to add a watermark in a given content have been proved to be Spread Spectrum (SS) approach and Side Information (SI).

As in spread spectrum communications, the former approach considers the

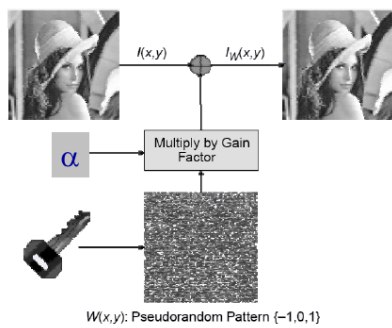


Figure 2.3: Spread spectrum technique

original content as a signal and the watermark as a noise that is spread over very many frequency bins so that the energy in any one bin is very small and

certainly undetectable.

The latter takes advantage of the fact that the original content is known at the embedder side (but unknown at the detector): this way the watermark can be modulated according to the original and the quantity of inserted data can be maximized.

Sometimes hybrid watermarking methods combining spread spectrum and side information concepts can be applied; they try to benefit from both the robustness and transparency of the spread spectrum methods and the increased data payload of the side information methods.

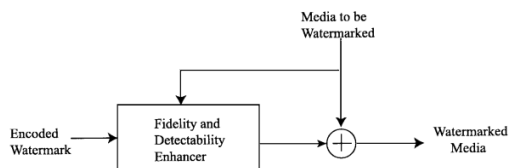


Figure 2.4: Side information technique scheme

2.1.3 Embedding domains

Host features modified during embedding can belong to

- spatial domain: the watermark is embedded by directly modifying the pixel values;



Figure 2.5: Spatial domain watermark insertion

- frequency domain: the image is transformed through a mathematical transformation, some coefficients are modified and finally the inverse transform is carried out;

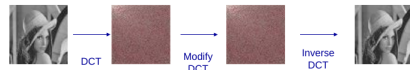


Figure 2.6: Frequency domain watermark insertion

- hybrid techniques: a block wise transform is applied, the image is divided into blocks and for each block a mathematical transformation is computed, some coefficients are modified and the inverse transform is done.

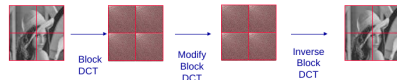


Figure 2.7: Hybrid technique

In stereoscopic video context the studies can also be structured in two other categories:

- view-based methods;
- disparity-based methods

according to the reference image in which the mark is actually inserted.

In Figure 2.8 the workflows of both methods are presented.

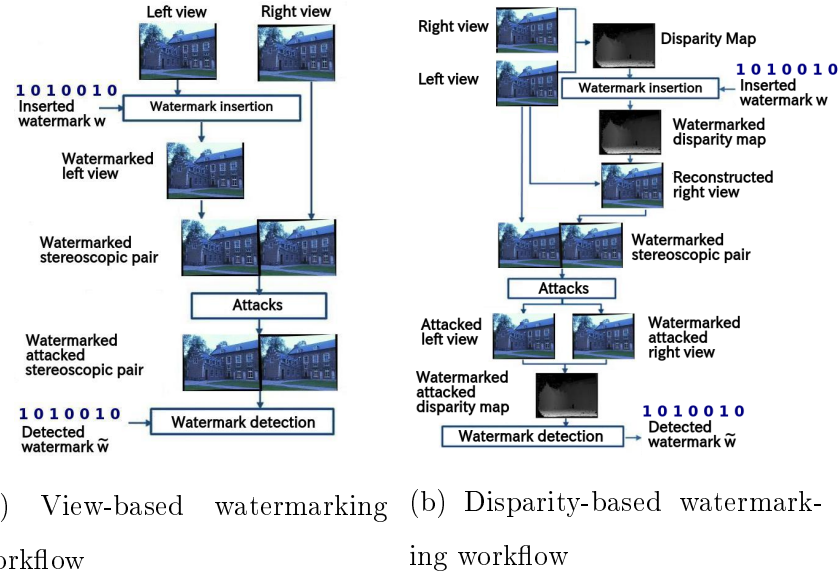


Figure 2.8: Stereoscopic video watermarking workflow

In this thesis due algoritmi di marchiatura presentati; il primo spaziale ss con rumore gaussiano etc.. il secondo ss nella frequenza additivo moltiplicativo...

data payload è ... la trasparenza è stata valutata con ... la robustezza è stata provata per view synthesis e compressione

Chapter 3

Frequency disparity-coherent watermarking

<<<< HEAD =====

Is now proposed a variant of the described watermarking process, which works in the frequency domain.

3.1 ALGORITMO DEL PROF

The strategy is based on the technique presented by Piva et al in "Improving DFT Watermarking robustness through optimum detection and synchronisation" [], where a watermarking algorithm for digital images operating in the frequency domain is presented: the method embeds a pseudo-random sequence of real numbers in a selected set of DFT coefficients of the image. Moreover, a synchronisation pattern is embedded into the watermarked image, to cope with geometrical attacks, like resizing and rotation. After embedding, the watermark is adapted to the image by exploiting the masking characteristics of the Human Visual System, thus ensuring the watermark

invisibility. (COPIATO DALL'INTRO DEL PROF, È LEGALE?)
 (immagine a blocchi del prof)

For the stereo watermarking task this process has been simplified and cut to the basic frequency watermarking.

3.1.1 Watermark embedding

In [] the watermark is embedded in a subset of DFT coefficients of the luminance Y .

Since a traslation of the scene will only change the phase values of the DFT, leaving unaltered the magnitude values, the watermak only concernes the latter, to achieve robustness against image traslation.

To garantee a blind detection system the number and position of the coefficient are fixed a priori: based on the size of the image to watermark, the coefficient are choosen in the medium frequencies of the spectrum to achieve a compromise between robustness and invisibillity.

The watermark embedding rule is the following:

$$y'_i = y_i + \alpha m_i y_i$$

where y'_i represents the watermarked DFT magnitude coefficient, y_i the corresponding original, m_i is a sample of the watermark sequence, and α is the watermark energy.

The inverted DFT is then applied to the obtained matrix to obtain the wa-termarked luminance Y' .

3.1.2 Watermark detection

To determine if a given image luminance Y either embedds or not the reference watermark in [] is used a threshold-based detection.

From the received image is extracted the luminance of which is computed the DFT transform; from the obtained magnitude matrix the right coefficients can be selected since their position is fixed a priori as said above.

Knowing the seed (in the shape of two strings, one numeric one alphanumeric) the watermark can be reproduced.

To verify if the selected coefficients have been altered with the watermark its used a statistical decision theory: two hypotheses are defined, the image contains the reference watermark (hypotheses H1) or the image does not contain this mark (hypotheses H0). Relying on Bayes theory of hypothesis testing, the optimum criterion to test H1 versus H0 is minimum Bayes risk; the test function results to be the likelihood ratio function L that has to be compared to a threshold:

- if $L > \lambda$, the watermark m^* is present;
- if $L < \lambda$, the watermark m^* is absent.

To choose a proper threshold, its been chosen to fix a constraint on the maximum false positive probability and the optimum decoder is designed refferring to the to the Neyman-Pearson criterion:

$$L(y) = \sum_{i=0}^{N-1} [-\beta \ln(1 + \alpha_m m_i^*)] + \sum_{i=0}^{N-1} \left[-\left(\frac{y_i}{\alpha_i(1 + \alpha_m m_i^*)} \right)^{\beta_i} + \left(\frac{y_i}{\alpha_i} \right)^{\beta_i} \right]$$

and

$$\lambda = 3.3 \sqrt{2 \sum_{i=0}^{N-1} \left[\frac{[(1 + \alpha_m m_i^*)^{\beta_i}]}{(1 + \alpha_m m_i^*)^{\beta_i}} \right]} + \sum_{i=0}^{N-1} \left\{ \frac{[(1 + \alpha_m m_i^*)^{\beta_i} - 1]}{(1 + \alpha_m m_i^*)^{\beta_i}} \right\} - \sum_{i=0}^{N-1} [\beta_i \ln(1 + \alpha_m m_i^*)]$$

In () $m^* = \{m_i^*\} i = 0, 1, \dots N - 1$ is the watermark, α_m the mean watermark energy, α_i and β_i are statistic parameters describing the probability density function shape of the magnitude of the watermarked DFT coefficient, y_i .

The values of this parameters are choosen by means of Maximum Likelihood criterion, based on the fact that the coefficients belonging to small sub-regions of the spectrum are characterised by the same statistic parameters and follows a Weibull distribution:

$$f(y_i) = \frac{\beta}{\alpha} \left(\frac{y_i}{\alpha}\right)^{\beta-1} \exp\left\{-\left(\frac{y_i}{\alpha}\right)^\beta\right\}$$

In summary, the detection process can be decomposed in the following steps:

- generation of the watermark m^* ;
- estimation of the parameters α, β into the regions composing the watermarked area of the spectrum;
- computation of $L(y)$ and λ ;
- comparison between $L(y)$ and λ ;
- decision.

The decoder can detect the watermark presence also in highly degraded images. In particular, the system is robust to sequences of different attacks, such as rotation, resizing, and JPEG compression, or such as cropping, resizing and median filtering.

3.2 Stereo watermarking algorithm

For the stereo-marking process its been taken under consideration a 512x512 subset of pixel of the image, in particular we focused in marking the part of

the scene which is common to both the left and right view.

IMMAGINE

The left view is then processed with the algorithm discribed above.

To watermark the right view the pattern is created ad-hoc: a signal of the watermak is generated using the phase of the left image and the phase of the reference watermark and the coefficients of the right view. This way the right view will be marked with its coefficient, but with the correct phase, and the corresponding pixel in the left and right view will present the same alteration, not to cause visual distorsions.

FORMULA CON TRASFORMATA DELLA SINISTRA MARCHIATA E POI DEL MARCHIO COSTRUITO PER LA DESTRA

The watermark is then brought back in the spatial domain with the inverse Fourier trasform, the image is warped according to the left-to-right disparity and added spatially to the right view.

3.3 Stereo detection algorithm

The detection of the watermark is performed with the detector implemented by Piva et al.

As for the embedding process, to the left view the algorithm is applied without changes, yet, for the right view detection some adaptations are needed.

First the detection algorithm computes the right-to-left disparity, then the right view is warped accordingly to ricreate the phase of the inserted watermark; to mantain the right phase the occluded zones are filled with the pixels of the recieved left view (taking under consideration that this little amount of image's pixel would not influence the detection). The created

image is then processed by the threshold-based detection algorithm.

»»»> ff8ca0de0d0a6deebfc456c21ed7df509e0c74c1

Chapter 4

Conclusions

Bibliography

- [1] Richard Hartley and Andrew Zisserman. Multiple View Geometry in Computer Vision, Cambridge University Press, 2000.
- [2] Lens Blur in the new Google Camera app
[http://googleresearch.blogspot.it/2014/04/
lens-blur-in-new-google-camera-app.html](http://googleresearch.blogspot.it/2014/04/lens-blur-in-new-google-camera-app.html)
- [3] Hewage, Chaminda TER, and Maria G.Martini. "Edges-based reduced-reference quality metric for 3D video compression and transmission." Selected Topics in Signal Processing, IEEE Journal of 6.5 (2012): 471-482.